SUPPLEMENTARY MATERIAL for *Critical Scaling Behaviors of Entanglement Spectra*

Qi-Cheng Tang[1] and Wei Zhu[1]

[1] *School of Science, Westlake University, Hangzhou 310024, China and Institute of Natural Sciences, Westlake Institute of Advanced Study, Hangzhou 310024, China*

I. CONFORMAL MAPPING OF QUANTUM QUENCHING A SEMI-INFINITE LINE

In order to introduce conformal mapping of global quantum quenching a semi-infinite line, first we need to represent the time evolution of density matrix $\rho(t)$ geometrically. The initial state $|\psi_0\rangle$ is chosen to be a short-range correlated state with correlation length β much less than the total system size, which can be considered as the ground state of a gapped Hamiltonian. In such a choice of initial state, the system is expected to be thermalized to a finite temperature $T = 1/\beta$ at long-time limit. A much clearer description is to assume that $|\psi_0\rangle$ can be written in the form $|\psi_0\rangle \sim e^{-\frac{\beta}{4}H_{\rm CFT}}|b\rangle$, where $|b\rangle$ is a conformal boundary state satisfying $(T(x)-\overline{T}(x))|b\rangle = 0$ [1, 2]. The factor $e^{-\frac{\beta}{4}H_{\rm CFT}}$ can be considered as a conformal mapping to the boundary state $|b\rangle$, giving the free energy $F = \frac{\pi cl}{6\beta^2}$. Technically, this is the origin of the appearing effective temperature in quantum dynamics, with $\rho(t) \sim e^{-iHt}e^{-\frac{\beta}{4}H_{\rm CFT}}|b\rangle\langle b|e^{-\frac{\beta}{4}H_{\rm CFT}}e^{+iHt}$. It is worth noting that this assumption of thermalization is very strong, and is not always true. The first insight is that the dynamical conserved free energy F has the same form with the finite-temperature thermalization [3, 4]. Moreover, the reduced density matrix is found to be exponentially close to a thermal Gibbs state, once the interval falls inside the horizon [1]. This fact strongly support the assumption we made. Based on above argument, we conclude that the global quench of a semi-infinite line can be described by as an infinite half-strip as shown in the left panel of Fig. **??**.

There, in fact, are more problems about the CFT calculation. The partial trace, which is required to calculate the reduced density matrix, will result the branch cut along $C = \left\{z = x + i\tau; x \in [0, l], \tau \in [-\frac{\beta}{4}, \frac{\beta}{4}]\right\}$. A small disc around the entangling points $z_0 = \left\{l + i\tau; \tau \in [-\frac{\beta}{4}, \frac{\beta}{4}]\right\}$ will lead to the *ultraviolet* divergence, and need be removed for regularization. In BCFT, a normal way is to introduce a boundary state $|a\rangle$, imposing around the entangling points. The regulator $|a\rangle$ will raise a boundary term known as the Affleck-Ludwig boundary entropy [5], which is also interesting to investigate. After this operation, the branch cut C becomes a surface connecting $|a\rangle$ and $|b\rangle$. It is important to note that the geometry of an infinite half-strip, including the branch cut caused by the partial trace, is topologically equivalent to an annulus (cylinder without boundaries). One can build a conformal mapping from the original infinite half-strip to an annulus, where the two boundary states $|a\rangle$ and $|b\rangle$ locate at two edges, connecting by the mapped branch cut. In such a geometry, the entanglement Hamiltonian can be considered as the generator of translation, so it could be a good choice.

The conformal mapping $w = f(z)$, from the infinite half-strip in z-plane to an annulus in w-plane, can be achieved through following there steps. First, by $\xi(z) = \sinh(\frac{2\pi z}{\beta})$, the infinite half-strip in z-plane is mapped to the right half part of ξ plane. Note that the entangling points z_0 are mapped to $\xi_0 = \xi(z_0)$. Second, we map the entangling points ξ_0 to $\mathrm{Re}(\xi_0') = (0, +\infty)$ by $\xi \to \xi'(\xi) = \frac{1+\overline{\xi_0}}{1+\xi_0} \cdot \frac{\xi+\xi_0}{\xi-\overline{\xi_0}}$. Third, applying $w(\xi') = \log(\xi')$, the right half ξ' plane is mapped to an annulus, with circumference 2π along $v = \mathrm{Im}w$ direction and width W along the $u = \mathrm{Re}w$ direction. The entangling points are simply removed, and the branch cut C is mapped to a curve $f(C)$ connecting the two edges of the annulus (the two boundary states $|a\rangle$ and $|b\rangle$).

II. CALCULATION OF THE ENTANGLEMENT HAMILTONIAN

Once we build up the conformal mapping $w = f(z)$ to an annulus, the entanglement Hamiltonian on original geometry can be written as a local integral over the Hamiltonian density $H(x)$. Remember that, on the annulus in the w-plane, the entanglement Hamiltonian H_E can be considered as the generator of translation along the $v = \mathrm{Im}w$ direction, as

$$H_E = -2\pi \int_{v=\text{const}} T_{vv} du = 2\pi \left[\int_{f(C)} T(w)dw + \int_{\overline{f(C)}} \overline{T}(\overline{w})d\overline{w} \right] , \tag{1}$$

where $f(C)$ is the branch cut C after conformal mapping, and the Hamiltonian density $T_{00} = -T_{vv}$ is written in terms of the holomorphic and anti-holomorphic components $T(w)$ and $\overline{T}(\overline{w})$. After mapping back to the z-plane, we have

$$H_E = 2\pi \left[\int_C \frac{T(z)}{f'(z)} dz + \int_{\overline{C}} \frac{\overline{T}(\overline{z})}{\overline{f'(z)}} dz \right] . \tag{2}$$

Using equation 2, it is straightforward to obtain the entanglement Hamiltonian $H_E(t)$ in our considered case (after analytical continuation $\tau \to it$), as

$$\begin{aligned} H_E(t) \ &= 2\beta \int_0^l \frac{\sinh\left[\frac{\pi(x-l)}{\beta}\right] \cosh\left[\frac{\pi(x-2t+l)}{\beta}\right] \sinh\left[\frac{\pi(x+l)}{\beta}\right] \cosh\left[\frac{\pi(x-2t-l)}{\beta}\right]}{\cosh\left(\frac{2\pi t}{\beta}\right) \sinh\left(\frac{2\pi l}{\beta}\right) \cosh\left[\frac{2\pi(x-t)}{\beta}\right]} T(x,t) dx \\ &+ 2\beta \int_0^l \frac{\sinh\left[\frac{\pi(x-l)}{\beta}\right] \cosh\left[\frac{\pi(x+2t+l)}{\beta}\right] \sinh\left[\frac{\pi(x+l)}{\beta}\right] \cosh\left[\frac{\pi(x+2t-l)}{\beta}\right]}{\cosh\left(\frac{2\pi t}{\beta}\right) \sinh\left(\frac{2\pi l}{\beta}\right) \cosh\left[\frac{2\pi(x+t)}{\beta}\right]} \overline{T}(x,t) dx . \end{aligned} \tag{3}$$

Simply taking $t = 0$ in equation 3, one can obtain the entanglement Hamiltonian in equilibrium

$$\begin{aligned} H_E(t=0) \ &= 2\beta \int_0^l \frac{\sinh\left[\frac{\pi(x-l)}{\beta}\right] \cosh\left[\frac{\pi(x-l)}{\beta}\right] \sinh\left[\frac{\pi(x+l)}{\beta}\right] \cosh\left[\frac{\pi(x+l)}{\beta}\right]}{\sinh\left(\frac{2\pi l}{\beta}\right) \cosh\left(\frac{2\pi x}{\beta}\right)} T_{00}(x) dx \\ &= \beta \int_0^l \frac{\sinh\left[\frac{\pi(x-l)}{\beta}\right] \sinh\left[\frac{\pi(x+l)}{\beta}\right]}{\sinh\left[\frac{2\pi(l+x)}{\beta}\right] + \sinh\left[\frac{2\pi(l-x)}{\beta}\right]} T_{00}(x) dx \\ &= \beta \int_0^l \left\{ \sinh^{-1}\left[\frac{2\pi(x-l)}{\beta}\right] - \sinh^{-1}\left[\frac{2\pi(x+l)}{\beta}\right] \right\}^{-1} T_{00}(x) dx . \end{aligned} \tag{4}$$

An important limit is to take $\beta \to \infty$, i.e. the critical ground state. In this case, the above equation becomes

$$H_E(t=0) = \int_A \frac{\pi(l^2 - x^2)}{l} H(x) dx , \tag{5}$$

which implies that the entanglement Hamiltonian on lattice geometry has a different structure with the CFT Hamiltonian.

For quenching to long time $t \to \infty$, the entanglement Hamiltonian

$$H_E(t \to \infty) \ = \ 2\beta \int_0^l \frac{\sinh\left[\frac{\pi(l-x)}{\beta}\right] \sinh\left[\frac{\pi(l+x)}{\beta}\right]}{\sinh\frac{2\pi l}{\beta}} T_{00}(x) dx \simeq \beta \int_0^l T_{00}(x) dx, \tag{6}$$

shares the same structure with CFT Hamiltonian up to a global factor β.

III. SCALING BEHAVIOR OF THE ENTANGLEMENT SPECTRUM AND ENTROPY: FROM THE WIDTH W OF THE MAPPED ANNULUS

In this section we show that the width W along the $u = \mathrm{Re}w$ direction of the mapped annulus plays important role in entanglement spectrum and entropy. The width W can be expressed as $W = \mathrm{Re}(\mathcal{W}) = \frac{1}{2}(\mathcal{W} + \overline{\mathcal{W}})$ with $\mathcal{W} = f(i\tau + l - \epsilon) - f(i\tau)$, where $f(z)$ is the conformal mapping from the original infinite half-strip to the annulus. A straightforward calculation (after analytical continuation to real time $\tau \to it$) gives

$$W = \log \left\{ \frac{2\sinh[\frac{2\pi(l-\epsilon/2)}{\beta}] \cosh(\frac{2\pi t}{\beta})}{\sinh(\frac{2\pi\epsilon/2}{\beta}) \sqrt{2\cosh(\frac{4\pi l}{\beta}) + 2\cosh(\frac{4\pi t}{\beta})}} \right\} \tag{7}$$

By taking the long-time lime $t \to \infty$, one can obtain its thermal value

$$W_{\mathrm{thermal}} \coloneqq W(t \to \infty) \ = \log \frac{\sinh[\frac{2\pi(l-\epsilon/2)}{\beta}]}{\sinh(\frac{2\pi\epsilon/2}{\beta})} \simeq \frac{2\pi}{\beta} l \tag{8}$$

The entanglement spectrum has the structure

$$E_i - E_j = \frac{2\pi^2(\Delta_i - \Delta_j)}{W_{\text{thermal}}} \simeq \frac{\beta\pi}{l}(\Delta_i - \Delta_j) \tag{9}$$

where E_i is the i-th level of entanglement Hamiltonian, and Δ_i is the level of i-th scaling operator. This also gives the long-time entropy as

$$S(t \to \infty) \simeq \frac{\pi c}{3\beta} l \tag{10}$$

For the time after reaching the saturate time $t = l$, W can be calculated by expanding to the term in t, straightforward algebra results

$$W(t > L) \simeq W_{\text{thermal}} - \frac{1}{2}\exp[-\frac{4\pi(t-l)}{\beta}] \tag{11}$$

which shows an exponential approaching to thermalization.

IV. LATTICE EFFECT: INHOMOGENEOUS EFFECTIVE TEMPERATURE β

The lattice effect plays important role in realization of dynamical CFT in lattice models. In this section, we show the effective temperature β is not uniform in lattice models, and strongly influences the behavior of dynamic entanglement spectrum. Consider the long time limit of the global quench, which is described by a conformal mapping to the annulus (cylinder without boundaries). The same geometry can also describe the finite-temperature thermalization. Recall that the thermal density matrix with inverse temperature β has the form

$$\rho_{\text{thermal}} = \frac{1}{Z}e^{-\beta H} = \frac{1}{Z}e^{-\sum_k \beta\epsilon_k \eta_k^\dagger \eta_k} \ , \tag{12}$$

where the (integrable) Hamiltonian can be diagonalized in the momentum space as $H = \sum_k \epsilon_k \eta_k^\dagger \eta_k$, and Z is the normalization factor. In our case, the reduced density matrix can be written in a similar form

$$\rho_A = \frac{1}{\tilde{Z}}e^{-\sum_k \varepsilon_k \xi_k^\dagger \xi_k} \ . \tag{13}$$

A direct comparison results a mode dependent effective temperature

$$\beta_k = \varepsilon_k/\epsilon_k \ . \tag{14}$$

The entanglement spectra $\{E_i\}$, i.e. the eigenvalues of $-\log[\rho_A]$, are simply

$$E_i = -\log\left[\frac{1}{\tilde{Z}}e^{-\sum_k \varepsilon_k n_k^i}\right] = \sum_k \varepsilon_k n_k^i + \log\left[\tilde{Z}\right] = \sum_k \beta_k \epsilon_k n_k^i + \log\left[\tilde{Z}\right] \ , \tag{15}$$

where the occupation numbers $n_k^i = 0, 1$. it is worth noting that, the renormalization factor $\tilde{Z}$, also the infinite order entropy $S_A^{(n\to\infty)} = E_1 = \log\left[\tilde{Z}\right]$, is effectively coupled to all modes in the momentum space, as $\tilde{Z} = \prod_k (1 + e^{-\varepsilon_k})$. However, the Schmidt gap $E_2 - E_1$ is always dependent only on one β_k corresponding to the lowest level in $\{\varepsilon_k\}$. The above argument explains why the effective temperature β is inhomogeneous at different levels of entanglement spectra. Moreover, through a derivation for Gaussian model, Calabrese and Cardy [6] show that β becomes independent on k when the correlation length (inverse mass) of the initial state $\to 0$. In our case, the mass term does not appear in the Hamiltonian directly, but the correlation length β decreases with increasing the distance between g and $g_c = 1$. Therefore an initial state with g far away from the critical point $g_c = 1$ is expected to give a better result in numeric, we will show that this is the case in following section.

V. DEPENDENCE ON THE INITIAL g OF THE GLOBAL QUENCH

In this section we present numeric of dynamic entanglement spectrum for different initial g. A finite-size scaling of the numerical results is shown in Fig. 1, and the same behaviors are observed in $g < 1$ ferromagnetic and $g > 1$

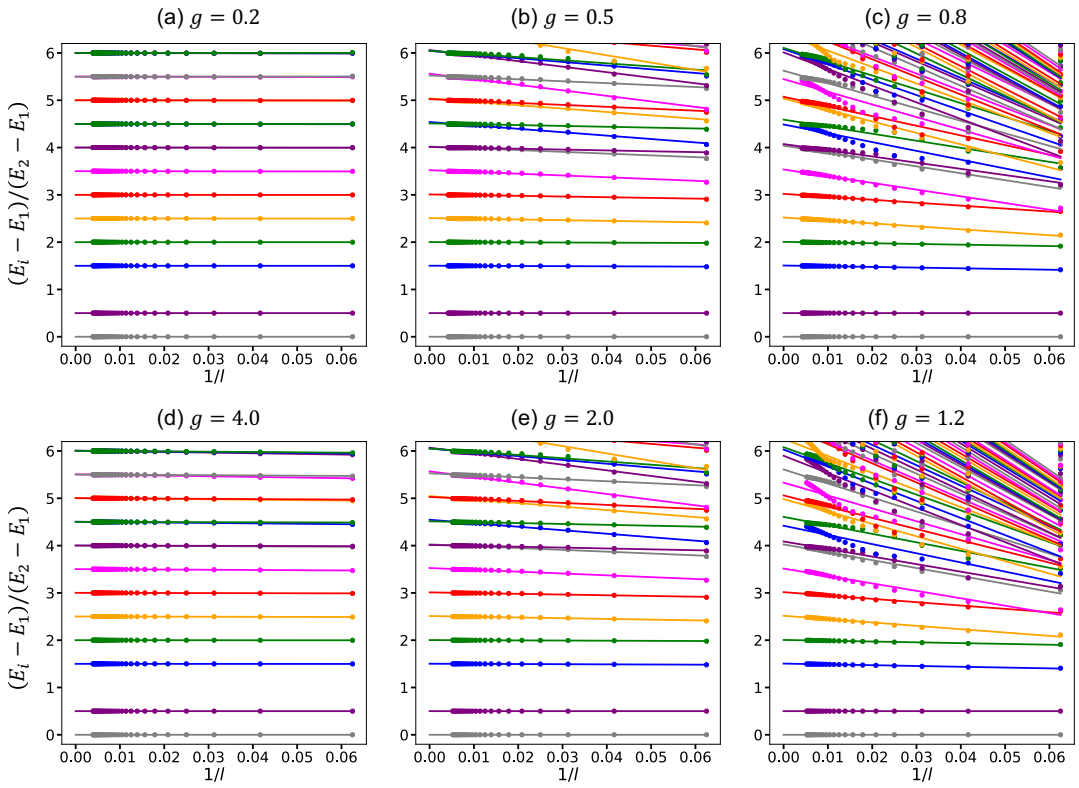

FIG. 1. Finite-size scaling of entanglement spectrum of dynamic equilibrium state for different initial g, with scaling function $F(l) = l^{-1}$. Both cases of ferromagnetic $g <$ (top) and paramagnetic $g > 1$ (bottom) are presented.

paramagnetic cases. As proposed in the last section and the main text, the convergence of entanglement spectrum exhibits a dependence on the initial condition (the distance between initial g and the critical point $g_c = 1$) of the global quench. The case of initial $g = 4$, presented in the main text, is a typical example of short-range correlated state with $\beta \ll L$. A very quick convergence in finite-size scaling can be directly observed. As shown in Fig. 1(a) and (d), when the initial g is far away from the critical point, the slope of scaling function $F(l) = l^{-1}$ shares the same value for different levels. When the initial g becomes closer to the critical point, especially when $g = 0.8$ and 1.2, the scaling function $F(l) = l^{-1}$ even not works for dynamic entanglement spectrum, since the initial state is no longer a short-range correlated state. In Table. I, we list the numerical results after finite-size scaling for different initial g. As we argued, when initial g is closer to the critical point, i.e. the gap is smaller, the numerical results are inconsistent with the CFT prediction.

TABLE I. A comparison of the operator content in dynamic equilibrium state during global quench from different initial g. Here Δ and D are the eigenvalue and degeneracy of i-th level respectively.

i-th level	sector	CFT		$g=0.2$		$g=0.5$		$g=0.8$		$g=1.2$		$g=2.0$		$g=4.0$	
		Δ	D	Δ	D	Δ	D	Δ	D	Δ	D	Δ	D	Δ	D
3	ϵ	3/2	1	1.50	1	1.50	1	1.51	1	1.51	1	1.50	1	1.50	1
4	I	2	1	2.00	1	2.00	1	2.01	1	2.01	1	2.00	1	2.00	1
5	ϵ	5/2	1	2.50	1	2.51	1	2.52	1	2.52	1	2.51	1	2.50	1
6	I	3	1	3.00	1	3.01	1	3.02	1	3.02	1	3.01	1	3.00	1
7	ϵ	7/2	1	3.50	1	3.52	1	3.54	1	3.52	1	3.53	1	3.50	1
8	I	4	2	4.00	2	4.01(2)	2	4.04(7)	2	4.03(9)	2	4.01(3)	2	4.00	2
9	ϵ	9/2	2	4.50	2	4.51(4)	2	4.49(59)	2	4.42(61)	2	4.51(5)	2	4.50	2
10	I	5	2	5.00	2	5.02(4)	2	5.04(7)	2	4.98(5.06)	2	5.03(5)	2	5.00	2
11	ϵ	11/2	2	5.50	2	5.52(6)	2	5.45(63)	2	5.33(61)	2	5.53(7)	2	5.50(1)	2
12	I	6	3	6.00	3	6.04(6)	3	6.01(11)	3	5.90(6.08)	3	6.05(7)	3	6.00(1)	3
13	ϵ	13/2	3	6.46(50)	3	6.54(7)	3	6.40	1	6.26	1	6.55(7)	3	6.50(1)	3
14	I	7	3	7.00	3	7.07	3	6.62(5)	2	6.55(60)	1	7.07(9)	3	7.01	3
15	ϵ	15/2	4	7.49(50)	4	7.57	4	6.93(7.09)	3	6.78	1	7.57(9)	4	7.50(1)	4
16	I	8	5	7.99(8.00)	5	8.06(9)	5	7.33	1	6.93(9)	2	8.06(10)	5	8.00(1)	5

[1] John Cardy, "Quantum quenches to a critical point in one dimension: some further results," Journal of Statistical Mechanics: Theory and Experiment **2016**, 023103 (2016).
[2] Pasquale Calabrese and John Cardy, "Quantum quenches in 1+1 dimensional conformal field theories," Journal of Statistical Mechanics: Theory and Experiment **2016**, 064003 (2016).
[3] H. W. J. Blöte, John L. Cardy, and M. P. Nightingale, "Conformal invariance, the central charge, and universal finite-size amplitudes at criticality," Phys. Rev. Lett. **56**, 742–745 (1986).
[4] Ian Affleck, "Universal term in the free energy at a critical point and the conformal anomaly," Phys. Rev. Lett. **56**, 746–748 (1986).
[5] Ian Affleck and Andreas W. W. Ludwig, "Universal noninteger "ground-state degeneracy" in critical quantum systems," Phys. Rev. Lett. **67**, 161–164 (1991).
[6] Pasquale Calabrese and John Cardy, "Quantum quenches in extended systems," Journal of Statistical Mechanics: Theory and Experiment **2007**, P06008 (2007).